ELSEVIER

Journal of Biomechanics 32 (1999) 453–460

JOURNAL OF BIOMECHANICS

A behavior-based inverse kinematics algorithm to predict arm prehension postures for computer-aided ergonomic evaluation

Xuguang Wang*

Institut National de Recherche sur les transports et leur Sécurité, 25 avenue François Mitterrand, Case 24, 69675 Bron, Cedex, France

Received in final form 17 January 1999

Abstract

In this paper, the computational problem of inverse kinematics of arm prehension movements was investigated. How motions of each joint involved in arm movements can be used to control the end-effector (hand) position and orientation was first examined. It is shown that the inverse kinematics problem due to the kinematic redundancy in joint space is ill-posed only at the control of hand orientation but not at the control of hand position. Based upon this analysis, a previously proposed inverse kinematics algorithm (Wang et Verriest, 1998a) to predict arm reach postures was extended to a seven-DOF arm model to predict arm prehension postures using a separate control of hand position and orientation. The algorithm can be either in rule-based form or by optimization through appropriate choice of weight coefficients. Compared to the algebraic inverse kinematics algorithm, the proposed algorithm can handle the non-linearity of joint limits in a straightforward way. In addition, no matrix inverse calculation is needed, thus avoiding the stability and convergence problems often occurring near a singularity of the Jacobian. Since an end-effector motion-oriented method is used to describe joint movements, observed behaviors of arm movements can be easily implemented in the algorithm. The proposed algorithm provides a general frame for arm postural control and can be used as an efficient postural manipulation tool for computer-aided ergonomic evaluation.

Keywords: Posture prediction; Inverse kinematics; Computer human model; Joint limits; Computer-aided ergonomic evaluation

1. Introduction

One of the main industrial applications of virtual human modeling and animation is to make an ergonomic evaluation of the man–machine interface of a product in a computer-aided design (CAD) environment at a very early stage of design (see review by Porter et al., 1993). For this, it is necessary to simulate human postures and movements under different task and environmental conditions. One of the problems encountered is so-called inverse kinematics. Usually, a task is specified in world space, but postures are defined by a set of joint angles. One natural question is how the constraints defined in a world space are transformed into a body joint space. However, the problem is ill-posed because the number of degrees of freedom (DOF) of the human body is generally greater than the number of equations imposed by the task. This means that there exists more than one possible solution for a task.

Much research has been done for the understanding of how humans control complex movements in human behavioral sciences and for the need of simulations in computer animation and robotics. It is well accepted that a solution to the ill-posed problems for the control of movements such as inverse kinematics is to find, in addition to biophysical and anatomical constraints, some other constraints to reduce the number of degrees of freedom to be controlled (Gielen et al., 1995). However, most solutions to these ill-posed problems proposed in human behavioral sciences remain conceptual (see for example Rosenbaum et al., 1995; Soechting et al., 1995) and cannot easily be implemented as a computer simulation algorithm. Meanwhile, it is difficult to integrate observed behaviors of the control of human movements in the methods proposed in robotics and computer animation of human figures (see Wang and Verriest, 1998a for a review). In addition, joint limits in most proposed inverse kinematics algorithms are

*Tel: 33-4-72-36-24-51; fax: 33-4-72-36-24-37; e-mail: wang@inrets.fr.

0021-9290/99/$ – see front matter
PII: S0021-9290(99)00023-8

simplified as linear inequalities, even for the shoulder joint.

Recently, Wang and Verriest (1998a) proposed a geometric method (as opposed to the algebraic method for pseudoinverses) for a four-DOF arm model to predict arm reaching postures. It was shown that the algorithm gives very natural-looking predictions in a large arm-reachable space. The objective of the present paper is to extend the algorithm to a seven-DOF arm model to predict arm prehension postures. Recent observations of the coordination of the proximal and distal joints involved in arm prehension movements (Wang, 1999) will be used to elaborate the rules and to validate the algorithm.

2. Method

The kinematic linkage of the human arm is supposed to be composed of the upper arm, lower arm and hand links connected by the shoulder, elbow and wrist joints. No translation is allowed at each joint. The shoulder is simplified into a ball and socket three-DOF joint, the elbow a two-DOF joint with flexion–extension $\mathbf{a}_{ef}$ and pronation–supination $\mathbf{a}_{ep}$ axes, and the wrist a two-DOF universal joint with flexion–extension $\mathbf{a}_{wf}$ and adduction–abduction $\mathbf{a}_{wa}$ axes. Consequently, the kinematic arm model studied in this work has seven DOF. Since the maximum number of the imposed independent parameters on the hand is six, the arm is kinematically redundant with respect to any hand task. For a complete determination of the arm posture from a given hand position and orientation, it needs at least one supplementary relation.

In order to better understand the nature of arm kinematic redundancy, we first examine how motions of each joint involved in arm movements can be used to control the hand position and orientation.

2.1. Hand position control

If $\mathbf{r}_w$ and $\mathbf{r}_w$ represent wrist and elbow position vectors, then the wrist velocity $\dot{\mathbf{r}}_w$ can be decomposed into two component vectors $\dot{\mathbf{r}}_{ws}$ and $\dot{\mathbf{r}}_{we}$, respectively, from the instantaneous rotations of the shoulder and elbow joints (Fig. 1)

$$\dot{\mathbf{r}}_w = \dot{\mathbf{r}}_{ws} + \dot{\mathbf{r}}_{we} = \mathbf{a}_s\dot{\theta}_s \times \mathbf{r}_w + \mathbf{a}_{ef}\dot{\theta}_{ef} \times (\mathbf{r}_w - \mathbf{r}_e), \quad (1)$$

where $\mathbf{a}_s\dot{\theta}_s$ and $\mathbf{a}_{ef}\dot{\theta}_{ef}$ are shoulder and elbow angular velocities with $\mathbf{a}_s$ and $\mathbf{a}_{ef}$ being the instantaneous rotation axis of the shoulder and the elbow flexion–extension axis. Since the forearm pronation–supination axis is supposed to be the longitudinal axis of the forearm, the wrist movement due to the elbow rotation $\dot{\mathbf{r}}_{we}$ is only contributed by elbow flexion–extension around its axis $\mathbf{a}_{ef}$. As the wrist movement due to shoulder rotation $\dot{\mathbf{r}}_{ws}$ must be within the wrist movement plane, formed by $\dot{\mathbf{r}}_w$ and

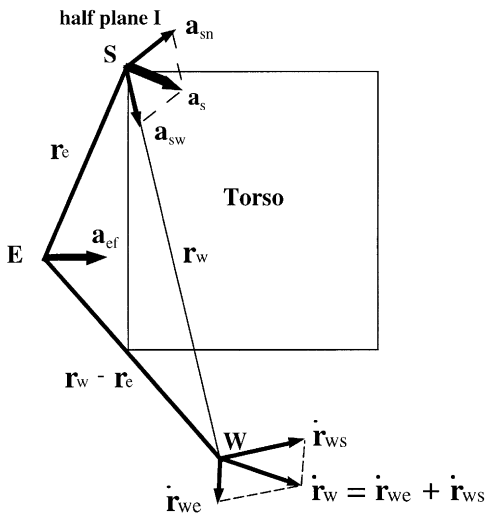

Fig. 1. Indeterminacy of arm pivoting about axis shoulder–wrist only from wrist motion. The shoulder, elbow and wrist joints are represented by S, E and W. The hand (wrist) velocity $\dot{\mathbf{r}}_w$ can be decomposed into two component vectors, one $\dot{\mathbf{r}}_{ws}$ contributed by the shoulder rotation and the another $\dot{\mathbf{r}}_{we}$ by the elbow. Knowing the elbow rotation flexion–extension axis $\mathbf{a}_{ef}$ and hand velocity $\dot{\mathbf{r}}_w$, the motions around the shoulder normal axis $\mathbf{a}_{sn}$ and the elbow axis $\mathbf{a}_{ef}$ are completely specified. Only the shoulder pivoting motion (self-motion) around the axis shoulder-wrist $\mathbf{a}_{sw}$ cannot be uniquely determined from a given hand velocity $\dot{\mathbf{r}}_w$.

$\dot{\mathbf{r}}_{we}$ (the direction of $\dot{\mathbf{r}}_{we}$ can be determined by the cross product of $\mathbf{a}_{ef}$ and the forearm link $\mathbf{r}_w - \mathbf{r}_c$), and must also be perpendicular to $\mathbf{r}_w$, it can be easily shown (Wang and Verriest, 1998a) that both $\dot{\mathbf{r}}_{ws}$ and $\dot{\mathbf{r}}_{we}$ are entirely determined from Eq. (1) for a given wrist velocity $\dot{\mathbf{r}}_w$. Accordingly, the elbow flexion–extension $\dot{\theta}_{ef}$ can be calculated from $\dot{\mathbf{r}}_{we}$. However, the shoulder rotation $\dot{\theta}_s$ cannot be uniquely determined from $\dot{\mathbf{r}}_{ws}$, since all lines passing through the shoulder joint S in a half-plane with its normal direction being $\dot{\mathbf{r}}_{ws}$ could be the shoulder instantaneous axis of rotation $\mathbf{a}_s$. If the shoulder angular velocity is decomposed along the axis shoulder–wrist $\mathbf{a}_{sw}$ and the axis $\mathbf{a}_{sn}$ perpendicular to $\mathbf{a}_{sw}$ in this half plane, only the shoulder angular velocity along $\mathbf{a}_{sn}$, which is the shoulder minimum angular velocity for a given $\dot{\mathbf{r}}_{ws}$, can be determined from $\dot{\gamma}_{ws}$. It is not possible to calculate the shoulder pivoting angle $\dot{\theta}_{sw}$. In fact, the shoulder pivoting axis passes through the wrist joint W, and the motion about this axis does not affect hand position and changes only hand orientation. Therefore, the shoulder motion $\dot{\theta}_{sn}$ about $\mathbf{a}_{sn}$ and the elbow flexion–extension $\dot{\theta}_{ef}$, which are responsible for the change of hand position, can be entirely determined from the wrist velocity $\dot{\mathbf{r}}_w$ (see Wang and Verriest, 1998a for details).

2.2. Hand orientation control

Apart from shoulder pivoting, the rotations about the axes of forearm pronation–supination $\mathbf{a}_{ep}$, wrist

flexion–extension $\mathbf{a}_{wf}$ and wrist abduction–adduction $\mathbf{a}_{wa}$ do not change wrist (hand) position, but change only hand orientation. For a variation of hand orientation $\mathbf{n}\dot{\theta}$, we have

$$\mathbf{n}\dot{\theta} - \mathbf{a}_{sn}\dot{\theta}_{sn} - \mathbf{a}_{ef}\dot{\theta}_{ef} = \mathbf{a}_{sw}\dot{\theta}_{sw} + \mathbf{a}_{ep}\dot{\theta}_{ep} + \mathbf{a}_{wf}\dot{\theta}_{wf} + \mathbf{a}_{wa}\dot{\theta}_{wa}, \quad (2)$$

where $\dot{\theta}_{sw}, \dot{\theta}_{ep}, \dot{\theta}_{wf}$ and $\dot{\theta}_{wa}$ are angular velocities about the axes $\mathbf{a}_{sw}$, $\mathbf{a}_{ep}$, $\mathbf{a}_{wf}$ and $\mathbf{a}_{wa}$. Note that relation (2) has three equations for four unknowns. This is to say that the inverse kinematics problem due to the kinematic redundancy in joint space is ill-posed only at the control of hand orientation. Therefore, the computational problem of inverse kinematics can be simplified if the control of hand position and orientation is separated.

2.3. Inverse kinematics of arm prehension movements

The inverse kinematics problem treated here is posed as follows: knowing the starting arm posture, the final hand position and orientation with respect to the object to be grasped, how can we calculate the final arm posture under the constraint of joint limits. The aim of the algorithm is to predict the elbow position, as only the elbow position is not restrained by the imposed geometric constraints. As shown before, Eq. (1) allows the determination of the shoulder minimal motion $\dot{\theta}_{sn}$ about $\mathbf{a}_{sn}$ and the elbow flexion–extension $\dot{\theta}_{ef}$ for a given wrist velocity $\dot{\mathbf{r}}_w$ (see Wang and Verriest, 1998a), and only the problem of hand orientation control is ill-posed. Since movements must be made within joint limits, joint limits are a very important constraint to be taken into account in inverse kinematics algorithms. In the appendix, a quantitative description of the range of motion for the shoulder, elbow and wrist joints is provided. Fig. 2 shows the excursion cones of the shoulder and elbow joints in a global torso-fixed coordinate system. Except for some extreme positions, joint limits do not generally allow a unique posture. In order to find a solution to Eq. (2), some heuristic behavioral rules will be elaborated from observations of real arm movements.

Recently, the influence of object orientations and joint limits on the control of arm prehension movements was experimentally investigated by Wang (1999). It was observed that forearm pronation is preferred to orient the hand compared to arm pivoting and that wrist angles are small and near the wrist neutral position after grasping (see also van der Vaart, 1995). These observations can be well explained by the principle of minimum work and minimum discomfort. On the one hand, the moment of inertia about the arm pivoting axis shoulder–wrist is much higher than that about the forearm pronation axis, thus leading a high cost in terms of work if arm pivoting mechanism is preferred to orient the hand (see also Soechting et al., 1995 for arm pointing movements).

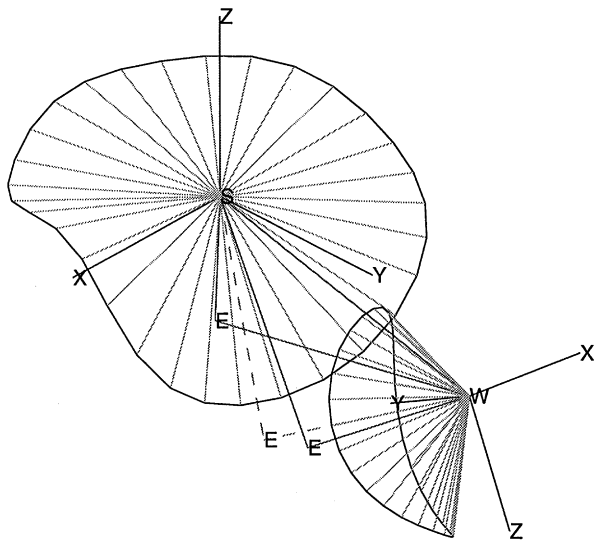

Fig. 2. Joint limits. The figure shows the excursion cones of the shoulder and elbow joints in a global torso-fixed coordinate system centered at the shoulder S, with $\mathbf{X}_t$, $\mathbf{Y}_t$ and $\mathbf{Z}_t$ being defined, respectively, aligned to the medial–lateral (M–L), posterior–anterior (P–A) and inferior–superior (I–S) anatomical directions. The upper arm link must be inside the shoulder excursion cone and its axial rotation angle must be within its maximum internal and external rotation limits. The same is true for the forearm link if forearm movements are observed from a hand-fixed coordinate system: the forearm must stay inside the wrist excursion cone and the forearm pronation–supination angle must be within its allowable values. From joint limits, two extreme arm postures can be determined for a given hand position and orientation. They are represented in solid line and the middle posture is represented in dotted line. Excursion cones of the shoulder and wrist joints are also shown in the figure.

On the other hand, a certain amount of arm pivoting allows the wrist to reduce its rotation angles, thus increasing the sensation of comfort (Wang, 1999; Cruse et al., 1990). Therefore, arm movements could result from a compromise between minimum work and minimum discomfort. The following assumptions are made explicitly based on the observed behaviors of arm prehension movements:

- At the beginning of the movement, the semi-pronated forearm and neutral wrist angles are imposed to assume an initial comfort position of forearm and wrist.
- When the hand is far from the object, only forearm pronation and shoulder pivoting are used to control hand orientation. Wrist movements, mainly through wrist flexion, are used to accompany the hand opening.
- When the hand is in the vicinity of the object, wrist motion and forearm pronation are used to assume the final control of hand orientation. The shoulder pivoting is only used to avoid joint limits.

The above assumptions can be integrated either in a rule-based algorithm or in an optimization-based algorithm. We assume that the final hand (wrist) position is

within arm-reachable space and the final hand orientation allows a solution within joint limits.

2.3.1. Rule-based algorithm

The main points of the proposed geometric algorithm in a rule-based form are illustrated as follows:

1. Take initial arm posture and final hand position and orientation as input parameters.
2. First impose an initial forearm and wrist comfort position (semi-pronated forearm and neutral wrist angles); then update the hand orientation.
3. Calculate the hand position error vector $\mathbf{D}_p$ comparing current wrist position $\mathbf{r}_w$ with final desired wrist position $\mathbf{r}_w^f$:$D_p = \mathbf{r}_w^f - \mathbf{r}_w = \mathbf{n}_p E_p$. If the hand position error E_p is beyond the tolerance limit, then impose a small hand position step $\Delta\mathbf{r}_w = \mathbf{n}_p\Delta_p$, calculate the shoulder minimal angular motion $\Delta\theta_{sn}$ and the elbow flexion–extension $\Delta\theta_{ef}$ from equation (1) (see Wang and Verriest, 1998a) and update the elbow position and hand orientation.
4. Calculate the orientation error vector $\mathbf{D}_o$ comparing current hand orientation $\mathbf{H}$ with final desired orientation $\mathbf{H}_f$: $\mathbf{D}_o = \mathbf{n}_o E_o$, where $\mathbf{n}_o$ and E_o are the screw axis and angle from rotation matrix $\mathbf{R} = \mathbf{H}_f\mathbf{H}^T$, and $\mathbf{H}^T$ is the transposed matrix of $\mathbf{H}$. If the hand orientation error E_o is beyond the tolerance limit, a small hand orientation step $\mathbf{n}_o\Delta_o$ is imposed to reduce the error:

- when the hand is far from the object ($E_p > 50$ mm for example), only forearm pronation $\mathbf{a}_{ep}\Delta\theta_{ep}$ and shoulder pivoting $\mathbf{a}_{sw}\Delta\theta_{sw}$ are used to control hand orientation with $\Delta\theta_{ep} = (\mathbf{n}_o\Delta_o)\mathbf{a}_{ep}$ and $\Delta\theta_{sw} = (\mathbf{n}_o\Delta_o)\,\mathbf{a}_{sw}$; update the elbow position and hand orientation.
- when the hand is in the vicinity of the object, only wrist flexion–extension and wrist abduction–adduction together with forearm pronation are used to assume the final control of hand orientation, whereas shoulder pivoting is supposed to not be applied; update the hand orientation $\mathbf{H} = \mathbf{R}(\mathbf{n}_o, \Delta_o)\mathbf{H}$, where $\mathbf{R}(\mathbf{n}_o,\Delta_o)$ is the rotation matrix corresponding to a rotation of Δ_o around the axis $\mathbf{n}_o$.

5. Check whether the upper arm is inside the shoulder excursion cone and whether the upper arm axial rotation angle is within its allowable range. If the shoulder joint limit is violated, apply a shoulder pivoting $\mathbf{a}_{sw}\Delta\theta_{sw}$ to bring the shoulder joint motion within its limits. In the same manner, if the wrist joint and forearm pronation–supination limits are violated, apply a shoulder pivoting $\mathbf{a}_{sw}\Delta\theta_{sw}$ to bring the wrist or forearm motion within their limits Update the elbow position.
6. Repeat 3, 4, and 5 until the hand position error E_p and orientation error E_o are within their chosen tolerance limits.

The arm pivoting mechanism is used here to avoid joint limits as in the case of an arm pointing task. The details of the algorithm for testing and avoidance of shoulder joint limits have been already explained in our previous paper (Wang and Verriest, 1998a), and shall not be repeated here. It is interesting to note, as stated by Korein (1985), that the sequence of motion types of the simplified kinematic arm linkage is symmetrical forwards and backwards from the proximal to distal ends: shoulder spherical motion, upper arm (humerus) axial rotation, elbow flexion–extension, forearm axial rotation (pronation–supination), wrist spherical motion. Taking advantage of this symmetry property, the same algorithm used for the shoulder joint can be applied for testing and avoidance of forearm pronation–supination and wrist joint limit violation. It is only necessary to express the wrist sinus and the elbow position in the hand-fixed coordinate system, and to treat the wrist joint like the shoulder (see also Korein, 1985).

2.3.2. Optimization-based algorithm

We suppose that a solution to Eq. 2 is obtained by minimizing the following cost function:

$$f = k_{sw}\dot{\theta}_{sw}^2 + k_{ep}\dot{\theta}_{ep}^2 + k_{wf}\dot{\theta}_{wf}^2 + k_{wa}\dot{\theta}_{wa}^2, \tag{3}$$

where k_{sw}, k_{ep}, k_{wf} and k_{wa} are weight coefficients. Since the wrist joint is simplified as a 2-DOF universal joint, the forearm-fixed orthogonal coordinate system can be used as the axes of rotation for forearm pronation–supination $\mathbf{a}_{ep}$, wrist flexion–extension $\mathbf{a}_{wf}$ and adduction–abduction $\mathbf{a}_{wa}$. Substituting the left-side of Eq. (2) by $\mathbf{n}_o\dot{\theta}_o$ and multiplying (2), respectively, by $\mathbf{a}_{ep}$, $\mathbf{a}_{wf}$ and $\mathbf{a}_{wa}$, the following can be obtained

$$\dot{\theta}_{ep} = \dot{\theta}_o n_{ep} - \dot{\theta}_{sw}a_{ep}, \quad \dot{\theta}_{wf} = \dot{\theta}_o n_{wf} - \dot{\theta}_{sw}a_{wf}$$

and $\dot{\theta}_{wa} = \dot{\theta}_o n_{wa} - \dot{\theta}_{sw}a_{wa}$,

where n_{ep}, n_{wf}, n_{wa}, a_{ep}, a_{wf}, a_{wa} are the projections of $\mathbf{n}_o$ and $\mathbf{a}_{sw}$ on the three mutually perpendicular axes $\mathbf{a}_{ep}$, $\mathbf{a}_{wf}$ and $\mathbf{a}_{wa}$. Through minimizing the function f in (3), the shoulder pivoting velocity $\dot{\theta}_{sw}$ can be easily obtained

$$\dot{\theta}_{sw} = \frac{k_{ep}n_{ep}a_{ep} + k_{wf}n_{wf}a_{wf} + k_{wa}n_{wa}a_{wa}}{k_{sw} + k_{ep}a_{ep}^2 + k_{wf}a_{wf}^2 + k_{wa}a_{wa}^2}\dot{\theta}_o. \tag{4}$$

Different control strategies can be elaborated through an appropriate choice of weight coefficients. If forearm pronation–supination is preferred to control hand orientation compared to shoulder pivoting, a higher coefficient associated with shoulder pivoting k_{sw} than the coefficient of forearm pronation–supination k_{ep} should be chosen. Since relatively small wrist motion was observed, two coefficients related to wrist motion should be more weighted than that of shoulder pivoting. As the motion range of wrist abduction–adduction is much smaller than that of wrist flexion–extension, a relatively high coefficient associated with wrist abduction–adduction should

be chosen to limit its movement. In the present work, the following weight coefficients are chosen by trial and error based on the experimental results in Wang (1998a): $k_{ep} = 1$, $k_{sw} = 1.5$, $k_{wf} = 2$ and $k_{wa} = 3$. Compared to the rule-based algorithm, only step 4 needs to be changed for the optimization-based algorithm.

Since the proposed algorithm is based on the analysis of joint instantaneous velocities, finite small steps Δ_p and Δ_o for wrist position and hand orientation should be used. To reduce calculation time, Δ_p and Δ_o could be variable, large at the beginning and small at the end approach. In the present work, the constant incremental steps for the control of hand position and orientation are used in the algorithm. They are chosen as $\Delta_p = 40$ mm and $\Delta_o = 5^\circ$, respectively. When arm pivoting along the axis shoulder-wrist is needed to avoid shoulder or wrist joint limits, a small pivoting angle $\Delta\theta_{sw} = 1^\circ$ or $\Delta\theta_{sw} = -1^\circ$ is imposed at step 5.

3. Experimental validation

In order to test and to validate the algorithm, the arm prehension postures measured in Wang (1999) are compared here with the predicted postures. Ten male subjects aged from 22–48 participated in the experiment. Each subject was instructed to grasp naturally a cylinder located at the shoulder level at a distance of about 50% of the length of the upper limb. Five different orientations in a fronto-parallel plane were tested: 0, 45, 90, 135, 180. The orientations 0 and 180 corresponded to a vertical cylinder with the thumb directed upwards and downwards, respectively, after grasping. The movements were measured using a VICON motion analysis system with four cameras at 50 Hz.

From the experimental data, starting arm posture and final hand position and orientation being taken as input parameters, the inverse kinematics algorithm is used to predict the corresponding final elbow position. Table 1 shows the distances between measured elbow positions and those predicted using the rule-based and optimization methods for all object orientations. One can see that the predictions by the rule-based and optimization methods are very similar. Except for one subject (subject 6) for whom the distances between predicted and measured elbow positions are systematically high, the error does not in general exceed 50 mm for either method, which can be considered acceptable for the computer-aided ergonomic application.

The middle elbow position between the two extreme positions restricted by joint limits is also compared with measured elbow positions in Table 1. It is interesting to note that the middle elbow position also gives a good prediction comparable to but higher than that of the proposed geometric algorithm in terms of absolute error. The middle elbow positions are systematically over-estimated (more elevated) for the object orientations 0, 45, 90, 135 (except for subject 5 at the orientation 45). This can be explained by the fact that only the constraint of joint limits is considered in the calculation of middle elbow positions and the principle of minimum work is not taken into account. More shoulder pivoting is used to orient the hand for the method of middle elbow position.

Table 1
Distances between calculated and measured elbow positions (mm)

Orientation	Rules-based algorithm					Optimization algorithm					Middle elbow position				
	0°	45°	90°	135°	180°	0°	45°	90°	135°	180°	0°	45°	90°	135°	180°
Subject 1	−53	−42	−31	−48	−50	−39	−35	−25	−33	−36	16	19	42	35	−31
Subject 2	17	21	−23	−32	−36	19	19	23	−29	−32	62	53	48	40	−16
Subject 3	−40	−34	−38	−44	−52	−35	−35	38	37	−35	31	32	58	42	−36
Subject 4	−27	−11	−24	−29	−21	−20	−11	−20	−28	−21	13	35	41	24	−13
Subject 5	−21	−36	−21	−31	21	5	−33	−16	27	21	10	−38	38	29	21
Subject 6	44	56	49	−61	−116	98	88	52	−41	−67	54	65	94	43	−49
Subject 7	−24	28	35	−35	34	−25	−27	37	36	−36	24	27	67	81	45
Subject 8	−21	31	43	−39	−50	38	38	43	35	−43	30	45	83	58	57
Subject 9	−33	−33	−33	−48	−46	−31	−34	−33	−43	−47	53	33	42	39	−35
Subject 10	−15	−10	−17	−22	−20	−15	−12	−18	−22	−20	68	62	62	37	23
Mean	−17	−3	−6	−39	−34	0	−4	8	−6	−24	36	33	58	43	−3
Std	28	35	34	12	42	43	41	33	35	31	21	29	19	16	37
Mean[a]	30	30	31	39	45	32	33	30	33	36	36	41	58	43	32
Std[a]	13	14	10	12	28	26	22	12	7	14	21	15	19	16	15

[a]Calculated from absolute values.

Three different methods are compared: rules-based algorithm, optimization method and middle elbow position with respect to two extreme positions limited by joint limits. The positive sign corresponds to the situation where a rotation about the shoulder–wrist axis is needed to make a predicted elbow position coincide with the corresponding measured position.

4. Some examples

As the heuristic rules used in the proposed algorithm are directly based on the observations from the experiment, it is not surprising to see that the predictions match quite well with the measured arm postures. It would be interesting to see how the algorithm works under other conditions. Since the object to be grasped was mainly located in the saggital plane crossing the shoulder in the experiment, some arm postures for other hand locations are simulated from different initial arm postures. As the rule-based and optimization methods give similar predictions, only the optimization method is used hereafter for examples. Fig. 3 shows simulated arm postures from two different initial positions (one being rest position and the other with arm directed laterally) for the same final hand position and orientation. It can be seen that two different final arm postures are obtained. This means that the algorithm is dependent of starting postures. In fact, the present inverse kinematics algorithm is a variation of the generalized pseudoinverse method (Wang and Verriest, 1998a) and has the property of end-effector trajectory dependence (Klein and Huang, 1983). Soechting et al. (1995) and Gielen et al. (1997) observed experimentally that starting postures have an influence on the final posture for a pointing task. It would be interesting to see experimentally to what extent the final posture is dependent of starting postures for a grasping task.

Since the inverse kinematics problem is resolved at the velocity level in the proposed algorithm, the final arm posture is obtained by reducing the gap between current and final hand position and orientation. A straight hand path in position and orientation is implicitly imposed. However, if the hand path is known as in the case of manipulating certain command controls (e.g. steering wheel, gear lever), the present algorithm is particularly useful in predicting the corresponding arm movement. Fig. 4 shows the succession of postures (movement) for a task of rotating steering wheel. Here initial hand position and orientation on the steering wheel are imposed and no relative motion between the hand

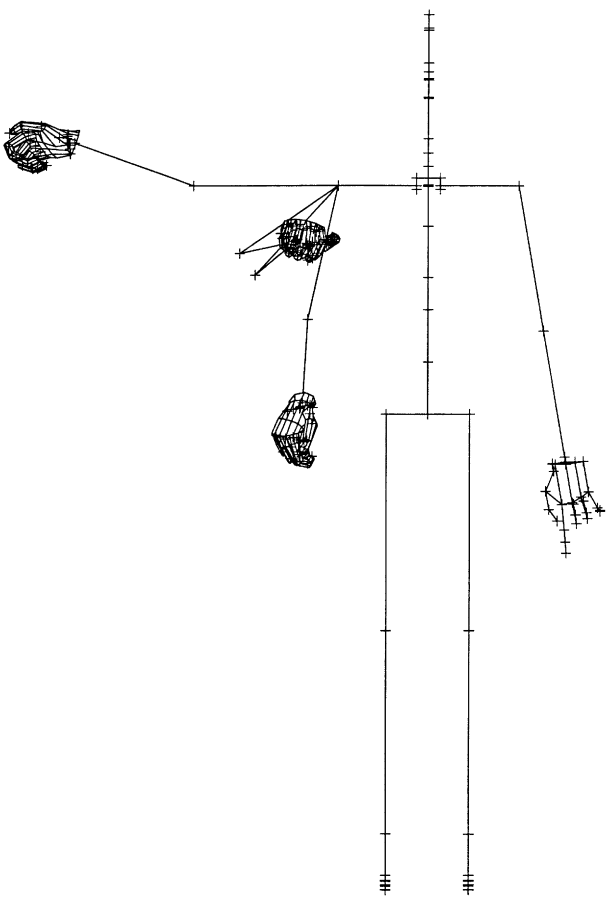

Fig. 3. Comparison of the simulated arm postures from two different initial positions (one being rest position and the other with arm directed laterally) for the same final hand position and orientation.

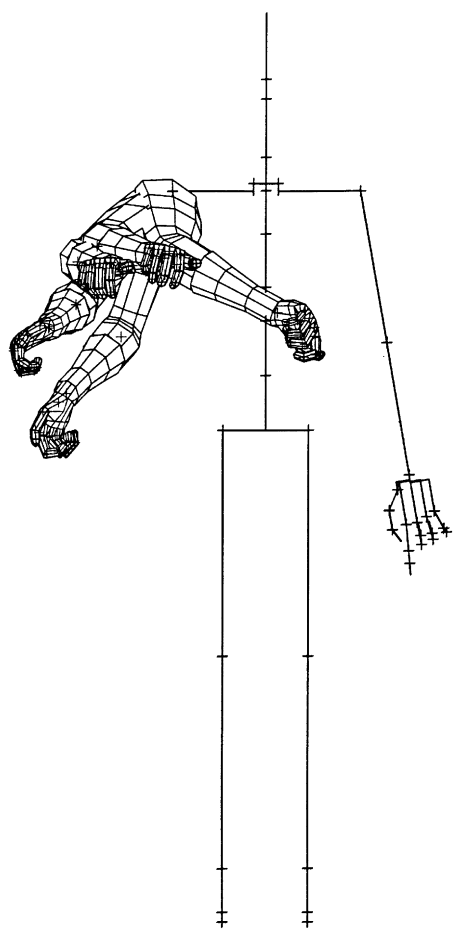

Fig. 4. Simulation of a succession of postures (movement) for a task of rotating steering wheel. Here initial hand position and orientation on the steering wheel are imposed and no relative motion between the hand and the steering wheel is supposed.

and the steering wheel is supposed. One can see that the algorithm predicts a reasonably natural-looking movement.

5. Discussion

In this paper, the previously proposed inverse kinematics algorithm was extended to a seven-DOF arm model to predict arm prehension postures, for which it needs the specification of both hand position and hand orientation. The algorithm can be either in rule-based form or by optimization through appropriate choice of weight coefficients. Compared to the algebraic generalized inverse kinematics algorithm, the present geometric algorithm can handle the non-linearity of joint limits in a straightforward way. In addition, no matrix inverse calculation is needed, thus avoiding the stability and convergence problems which often occur near a singularity of the Jacobian. Since an end-effector motion-oriented method is used to describe joint movements, observed behaviors of arm movements can be easily implemented in the proposed algorithm.

It should be noted that the rules used in the algorithm to solve the redundancy problem posed at the control of hand orientation (Eq. (2)) are mainly based on the experimental results by Wang (1999). Remember that the subjects were simply asked to grasp a cylinder for that experiment. The rules may not be appropriate to describe arm movements for other tasks, for instance, a task of grasping and rotating an object with force. Van der Vaart (1995) observed from arm movements in operating rotary controls that arm postures may also depend on the rotation magnitude to be carried out: different arm postures may be adopted to rotate the same rotary control from the same initial arm posture if different amounts of rotation are imposed. Soechting et al. (1995) reported that starting postures have an influence on final postures for a pointing task. Although the present algorithm predicts different postures from different initial arm positions for the same final hand position and orientation, it remains to be verified whether predictions match experiments. Knowing that the control of postures and movements is a very complex problem due to the redundancy of the human musculoskeletal system, the aim of the inverse kinematics algorithm is not to predict exact postures but to provide a general frame for arm postural manipulation allowing less manual intervention.

As conclusions, the present algorithm provides a general frame for the postural control of the arm, in which non-linear joint limits can be handled easily and heuristic behavioral rules can be integrated in a straightforward way. It can be used as an efficient postural manipulation tool for computer-aided ergonomic evaluation.

Appendix A. Three-dimensional range of motion of the joints involved in arm movements

A.1. Shoulder joint

The shoulder joint sinus, also called shoulder excursion cone (Dempster, 1965), was quantified by Engin and Chen (1986) based on a statistical in vivo database from a male adult population. Recently, Wang et al. (1998) extended their work and quantified the upper arm axial motion range for the same population. Therefore, the three-dimensional maximum range of motion of the shoulder joint has been completely modeled.

A.2. Elbow joint

The range of motion of elbow joint flexion–extension and forearm pronation–supination is supposed to be independent of the shoulder and wrist angles, and is characterized by an inequality $\theta_{\inf} \leqslant \theta \leqslant \theta_{\sup}$. Different values were reported in the literature especially for the range of motion of forearm pronation–supination (van der Vaart, 1995). Since the shoulder joint limit database is based on a population of male adults, following values are taken here: the elbow has a maximal value of 0° for extension and a maximal value of 142° for flexion, and the forearm has a maximal value of 90° for supination and a maximal value of 80° for pronation.

A.3. Wrist joint

As far as the range of motion of the wrist joint is concerned, the wrist joint sinus (excursion cone) was recently quantified for a male adult population (9 healthy subjects aged from 23 to 43, see Wang, 1998). An ellipse was found appropriate to fit maximum wrist flexion–extension angles $\theta_f^{\lim}$ in terms of maximum wrist abduction–adduction angles $\theta_a^{\lim}$:

$$\frac{[(\theta_f^{\lim} - x_0)\cos\alpha + (\theta_a^{\lim} - y_0)\sin\alpha]^2}{a^2} + \frac{[-(\theta_f^{\lim} - x_0)\sin\alpha + (\theta_a^{\lim} - y_0)\cos\alpha]^2}{b^2} = 1$$

where a, b, α, x_0, y_0 are the five parameters of ellipse with following values (all in degrees),

A	B	α	x_0	y_0
62.5	24.2	99.7	5.6	−8.8

The wrist may rotate on average from -70 to 60° in flexion–extension and from -20 to 30° in abduction–adduction. Fig. 2 shows the excursion cones of the shoulder and wrist joints in a torso-fixed coordinate system.

References

Cruse, H., Wischmeyer, E., Brüwer, M., Brockfeld, P., Dress, A., 1990. On the cost functions for the control of the human arm movement. Biological Cybernetics 62, 519–528.

Dempster, W.T., 1965. Mechanisms of shoulder movements. Archives of Physical Medicine and Rehabilitation 46(1–A), 49–69.

Engin, A.E., Chen, S.M., 1986. Statistical data base for the biomechanical properties of the human shoulder complex – I: Kinematics of the shoulder complex. Journal of Biomechanical Engineering 108, 215–221.

Gielen, C.C.A.M., Van Bolhuis, B.M., Theeuwen, M., 1995. On the control of biologically and kinematically redundant manipulators. Human Movement Science 14, 487–509.

Gielen, C.C.A.M, Vrijenhoek, E.J., Flash, T., Neggers, S.F.W., 1997. Arm position constraints during pointing and reaching in 3D space. Journal of Neurophysiology 78, 660–673.

Hollerbach, J.M., Suh, K.C., 1985. Redundancy resolution of manipulators through torque optimization. In: Proceedings of the 1985 IEEE International Conference on Robotics and Automation, Computer Soc. Press, Silver Spring, pp. 1016–1021.

Klein C.A., Huang, C.H., 1983. Review of pseudoinverse control for use with kinematically redundant manipulators. IEEE Transactions Systems, Man, Cybernetics SMC-13, 245–250.

Korein J., 1985. A Geometric Investigation of Reach, MIT Press, Cambridge, MA.

Porter, J.M., Case, K., Freer, M.T., Bonney, M.C., 1993. Computer aided ergonomics design of automobiles. In: Karwowski, (Ed.), Automotive Ergonomics, Taylor and Francis, London, pp. 43–77.

Rosenbaum, D.A., Loukopoulos, L.D., Meulenbroek, R.G.J., Vaughan, F., Engelbrecht, S.E., 1995. Planning reaches by evaluating stored postures. Psychological Review 102, 28–67.

Soechting, J.F., Buneo, C.A., Herrmann, U., Flanders, M., 1995. Moving effortlessly in three dimensions: does Donders, law apply to arm movement? The Journal of Neuroscience 15(9), 6271–6280.

Van der Vaart, A.J.M., 1995. Arm movements in operating rotary controls. Delft University Press.

Wang X.G., 1998. Quantification en 3D du cone de circumduction du complexe articulaire du poignet. XXIIIth Congres of Société de Biomécanique, Lyon, France, 17–18 September 1998. Archives of Physiology and Biochemistry, vol. 106, (Supplement B), pp. 96.

Wang, X.G., 1999. Three-dimensional kinematic analysis of influence of hand orientation and joint limits on the control of arm posture and movement. Biological Cybernetics, Accepted for publication.

Wang, X.G., Verriest, J.P., 1998a. A geometric algorithm to predict the arm reach posture for computer-aided ergonomic evaluation. The Journal of Visualization and Computer Animation 9, 33–47.

Wang, X.G., Maurin, M., Mazet, F., De Castro Maia, N., Voinot, K., Verriest, J.P., Fayet, M., 1998b. Three-dimensional modeling of the motion range of the upper arm axial rotation. Journal of Biomechanics 31(10), 899–908.